

Vortex-induced negative magnetoresistance and peak effect in narrow superconducting films

D. Y. Vodolazov*

Institute for Physics of Microstructures, Russian Academy of Sciences, 603950, Nizhny Novgorod, GSP-105, Russia

(Received 4 June 2013; revised manuscript received 10 July 2013; published 25 July 2013)

In the framework of the Ginzburg-Landau model, it is shown that narrow superconducting films with width $w \simeq 3\text{--}8\xi(T)$ [$\xi(T)$ is a temperature-dependent coherence length] exhibit unusual transport properties. In the absence of bulk pinning, its critical current I_c nonmonotonically depends on perpendicular magnetic field H and has one minima (dip) and one maxima (peak) at some magnetic fields. At currents $I \ll I_c(H)$, the finite magnetoresistance $R(H)$ of such a sample due to thermoactivated vortex hopping via edge barriers also shows both local maxima (peak) and minima (dip) nearly at the same magnetic fields. In narrower films, such an effect is absent due to absence of the vortices and in wider films the effect is weaker due to increased vortex-vortex interaction. The finite length of the film produces additional periodic variation in both $I_c(H)$ and $R(H)$ because of discrete changes in the number of the vortices, which is superimposed on the above-mentioned nonmonotonic dependence. The obtained results are directly related to many experiments on narrow superconducting films/bridges where such nonmonotonic dependencies $I_c(H)$ and $R(H)$ were observed.

DOI: 10.1103/PhysRevB.88.014525

PACS number(s): 74.25.Op, 74.20.De, 73.23.–b

I. INTRODUCTION

It is well known that mesoscopic superconductors [with lateral and transverse sizes comparable with temperature-dependent coherence length $\xi(T)$] have transport characteristics (critical current I_c and resistance R) which nonmonotonically depend on applied magnetic field H . Probably the most familiar example is a Little-Parks effect when the resistance of the hollow superconducting cylinder (so-called double connected system) varies periodically with H because of the change in vorticity.¹ Variations of the critical current in the double connected system (superconducting ring) are found in Refs. 2 and 3, while the same effect in single connected superconducting samples (squares, triangles, etc.) is experimentally observed in Refs. 4–7. Physically, both in single connected and double connected geometries, the effect is connected with adding to the screening current j_{scr} , induced by the external magnetic field, the current which flows around the vortex (or current created by the fluxoid in the ring and hollow cylinder). These currents cancel each other (fully or partially) and it results in periodic variation of I_c and R with H . In a large-scale system (with sizes $\gg \xi$), the effects practically disappear (amplitude of variation of I_c and $R \rightarrow 0$) because the current induced by the single vortex decays fast far from the vortex core.

In this paper, we show that thin narrow superconducting films with width $3\xi \lesssim w \lesssim 8\xi \ll \Lambda$ ($\Lambda = 2\lambda^2/d$, where λ is the London penetration depth and $d < \lambda$ is a thickness of the film) placed in perpendicular magnetic field have nonmonotonic $I_c(H)$ and $R(H)$ although their length may go to infinity. As compared with the mesoscopic samples, the effect is mainly connected not with a change in the number of the vortices, but with the appearance of the vortex row in the film when the magnetic field increases.

Let us first discuss what the minimal width is of the film in which this effect may exist. In Ref. 8, it is shown (in the framework of the Ginzburg-Landau model) that vortices may appear only in the films with width $w^* \gtrsim 1.8\xi(T)$ at finite magnetic field and they do not penetrate to the narrower film at any magnetic field smaller than H_c (H_c is a critical field at

which the superconductivity vanishes and H_c is equal to third critical field H_{c3} when $w \gg \xi$ and $H_c \sim 1/w$ for the films with $w \ll \xi$). Sometimes in the literature a different critical width $\tilde{w}^* \simeq 4.4\xi$ is used which follows from numerical calculations for the superconducting bridge attached to a bulk electrode.⁹ Note that the last result is found in the case when $H = 0$ and the state with a vortex sitting in the center of the film (when $I \rightarrow 0$) is a *saddle-point* state. In Refs. 10 and 11, it is argued that the energy of such a vortex state U_{vortex} practically coincides with the energy of the Langer-Ambegaokar U_{LA} saddle-point state¹² [in this state the order parameter vanishes along the line connecting opposite edges of the film (see inset in Fig. 1 of Ref. 11)] when $w \lesssim 4.4\xi$. In wider films, $U_{\text{vortex}} < U_{\text{LA}}$ and it takes less energy to create a vortex than a LA state at $I \ll I_{\text{dep}}$ [but still there is a range of the currents very close to depairing current I_{dep} where $U_{\text{vortex}} > U_{\text{LA}}$ even for films with $w \gg 4.4\xi$ (Ref. 11)].

When $w > w^*$, it is energetically favorable to have vortices in the *ground* state of the film at magnetic fields $H_{c1} < H < H_c$, but as a *metastable* state the vortices also could exist at lower fields $H_0 < H < H_{c1}$ due to finite-energy barrier for vortex exit [it originates from trapping of the vortex by the screening current $j_{\text{scr}}(H)$]. In the the London model, magnetic fields H_{c1} and H_0 were calculated in several works,^{13–15} and for a set of widths they were calculated numerically in the Ginzburg-Landau (GL) approach in Ref. 16.

The increase of I_c with appearance in the narrow film, one disperse vortex row (with intervortex distance $a \gg w$) was theoretically predicted by Shmidt¹⁷ more than 40 years ago in the framework of the London model. Physically, this effect was explained by increased trapping of the vortices by $j_{\text{scr}}(H)$ when the magnetic field increases and it is necessary to increase transport current to overcome this force. In Ref. 17, it was argued that after reaching maximal value the critical current should decay at larger magnetic fields due to the suppression of superconductivity by magnetic field and hence it should be peak in dependence $I_c(H)$ (see curve I_c^a in Fig. 1).

Much later in Refs. 18 and 19 it was found that entrance of second, third, and subsequent vortex rows to the film leads to

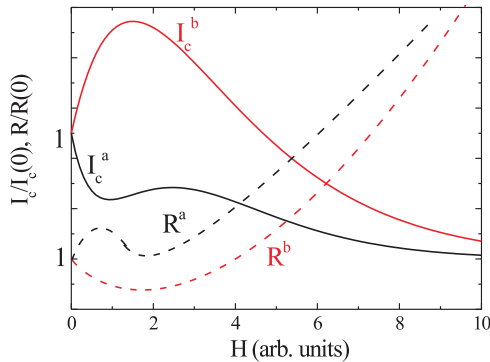


FIG. 1. (Color online) Sketch of two types of nonmonotonic dependence $I_c(H)$ (solid curves) and related with them $R(H)$ (dashed curves) observed in many experiments on narrow superconducting films.

additional dips (and peaks) in dependence $I_c(H)$. In the case of relatively wide film (in the sense that $\xi \ll w < \Lambda$), one may use continuous approach with coordinate-dependent vortex density when the number of vortex rows is large. This approach was utilized by Maksimova²⁰ and it predicted monotonic decay of critical current in increasing magnetic fields.

Experimentally, dependence $I_c(H)$ was studied in various narrow superconducting films. One dip/peak in $I_c(H)$ was found for Nb film with $w \sim 4-5\xi$,²¹ several dips/peaks were present for the film with $w \sim 7-10\xi$,²² and no dips and a monotonic $I_c(H)$ were observed for Nb and NbN films with $w \gg \xi$ in Refs. 14, 23, and 24. It is important that in these experiments the effect of bulk pinning was negligible at low magnetic fields, and dependence $I_c(H)$ was governed only by edge/surface barrier effect (impact of bulk pinning in the film with edge barrier for vortex entry/exit was discussed in Refs. 25 and 26 and analytically it was studied in Refs. 27 and 28).

Note that enhancement of I_c with an increase of H was also observed in narrow superconducting wires with width $w \lesssim \xi$,^{29,30} where one can not expect the effect of vortices. Qualitatively, the dependence $I_c(H)$ had a form which is different from the above-mentioned dependence (see curve I_c^b in Fig. 1). We believe that enhancement of I_c found in Refs. 29 and 30 has a different origin (for discussion of this behavior see Refs. 31–33) and it is not connected with an appearance of the vortices in the film/wire.

When I_c is a nonmonotonic function of H , one may expect that resistance also changes nonmonotonically with H . Indeed, at current larger than $I_c(H)$, finite resistance appears due to vortex motion and just above $I_c(H)$ one may write $R \sim [I - I_c(H)]$ (assuming that there is not voltage jump at $I = I_c$). Therefore, if one fixes current I and changes I_c by applying magnetic field, then variations in $I_c(H)$ will be directly reflected in variations of $R(H)$. This problem for narrow film was numerically studied in recent work³⁴ (using the time-dependent Ginzburg-Landau equation) and authors found nonmonotonic $R(H)$.

A more complicated question is the finite resistance below I_c . If one uses the concept of the energy barrier U for the vortex entry/exit to/from the superconductor then, by definition, these barriers vanish at $I = I_c(H)$. Due to thermoactivation, the

vortex has finite probability P to enter/exit the superconductor even when the height of the barriers is finite [at $I < I_c(H)$] and passage of the vortex through the superconductor leads to the voltage pulse and finite resistance. In the simplest model, one may write that near the critical current $U \sim U_0(1 - I/I_c)^m$ (for example, $m \simeq 1$ for narrow film at zero magnetic field¹¹) and because $P \sim \exp(-U/k_B T)$ the resistance is proportional to $\sim \exp[-U_0(1 - I/I_c)^m/k_B T]$. Therefore, variations of I_c in magnetic field should be reflected in variations of R even at $I < I_c$ (stress here that I_c in the above discussion is a theoretical critical current in the absence of fluctuations).

Experimentally, nonmonotonic (negative) magnetoresistance in narrow superconducting films/wires was observed in many experiments.^{29,35–46} As in the case with $I_c(H)$, one can distinguish two types of dependence $R(H)$. In one set of experiments,^{29,41–46} dependence $R(H)$ had a dip at low magnetic fields and then resistance reached a normal-state value at large H (see curve R^b in Fig. 1). Such a behavior was mainly observed in quasi-one-dimensional (quasi-1D) films/wires with width $w \gtrsim \xi$ where no vortices can exist. At the moment, there are several theories^{31,33,47–50} which explain this effect by different mechanisms (for comparison of theoretical models, see Refs. 33 and 47).

In another set of experiments,^{35–40} $R(H)$ had qualitatively different behavior. At weak magnetic fields, first there was a peak in $R(H)$ which was followed by the dip (see curve R^a in Fig. 1). Besides, as in case of corresponding $I_c(H)$, there could be several dips/peaks in $R(H)$.^{35,37–39} Sometimes, the oscillations of $R(H)$ with much smaller amplitude and shorter period could be superimposed on this nonmonotonic behavior^{37,38} and they were related to the change by one in the number of the vortices in the film.³⁷

These experiments motivate us to calculate the dependencies $I_c(H)$ and $R(H)$ for narrow films in a wide range of widths. Contrary to previous theoretical works on this subject, we use the Ginzburg-Landau approach because it takes into account suppression of the superconducting order parameter by the screening/transport current (which is important when the critical current is close to the depairing current or magnetic field is close to H_c) and the effect of the finite-size vortex core, which are absent in the the London model and which are important from a quantitative point of view. Besides, the GL model automatically correctly takes into account vortex-vortex interaction in the presence of edges (via boundary conditions for superconducting order parameter) and resolves the question about stability of static vortex configurations in the film with transport current. Previously, $I_c(H)$ was already calculated in the GL model for narrow film (for restricted set of widths) and a dip/peak in dependence $I_c(H)$ was found in Refs. 51 and 52, but its origin was not studied.

To calculate the magnetoresistance $R(H)$, we find the energy barriers for the vortex entry U_{en} and vortex exit U_{ex} both in the presence and in the absence of the vortices in the film in the limit when $I \rightarrow 0$. For this purpose, we find the solution of the Ginzburg-Landau equation which corresponds to the saddle-point state. The magnetoresistance is estimated by using the Arrhenius law $R(H) \sim \exp(-U_{\text{max}}/k_B T)$, where U_{max} is a maximal energy barrier at given magnetic field $U_{\text{max}}(H) = \max\{U_{\text{en}}, U_{\text{ex}}\}$. Comparison of our results with existing experiments showed good qualitative and sometimes

quantitative agreement. The possible reasons for quantitative disagreement are discussed.

The paper is organized as follows. In Sec. II, we present the results for $I_c(H)$ and compare them with existing theories and experiments. In Sec. III, we present results for $R(H)$ and compare them with the experiments. In Sec. IV, we conclude our main results.

II. DEPENDENCE OF THE CRITICAL CURRENT ON MAGNETIC FIELD

A. Model

In numerical calculations, we mainly use the length of the film $L = 40\xi$ and vary the width from $w = 2\xi$ up to 20ξ . At the ends of the film, we apply normal-metal–superconductor (NS) boundary conditions to inject the current to the superconductor. To avoid the effect of these NS contacts on the vortex distribution and stability of the superconducting state, we locally enhance critical temperature (on the distance 2.5ξ) near the ends. It leads to enhanced order parameter near the ends, which partially mimics the effect of bulk leads to which wire/film/bridge is usually attached in the experiment. We check that these places lose the superconducting properties at larger currents than the main part of the film.

The critical current is determined as a current at which vortex motion starts (without fluctuations) and voltage drop across the central part of the film becomes nonzero. Fluctuations (if they are strong enough) may provide switching of the superconductor to the resistive state at $I < I_c$, but because their probability is roughly proportional to $\exp\{-U_0[I_c(H) - I]^m\}/k_B T$ (see discussion in the Introduction) one may expect that $I_c(H)$ in the presence of fluctuations follows $I_c(H)$ in the absence of fluctuations (if $U_0/k_B T \gg 1$ and these fluctuations are relatively rare events).

In the model, we assume that the London penetration depth λ is much larger than the width of the film and hence one can neglect the magnetic field which is induced by the transport and screening currents. It considerably simplifies the calculations because we have to solve only the two-dimensional (2D) Ginzburg-Landau equation for the superconducting order parameter $\Delta = |\Delta|\exp(i\phi)$:

$$\begin{aligned} & \frac{\pi\hbar}{8k_B T_c} \left(\frac{\partial}{\partial t} + 2ie\varphi \right) \Delta \\ & = \xi_{\text{GL}}^2 \left(\nabla - i \frac{2e\mathbf{A}}{\hbar c} \right)^2 \Delta + \left(1 - \frac{T}{T_c} - \frac{|\Delta|^2}{\Delta_{\text{GL}}^2} \right) \Delta. \end{aligned} \quad (1)$$

In Eq. (1), $\xi_{\text{GL}}^2 = \pi\hbar D/8k_B T_c$, $\Delta_{\text{GL}}^2 = 8\pi^2(k_B T_c)^2/7\zeta(3)$, and D is a diffusion coefficient. Vector potential \mathbf{A} has only one component $\mathbf{A} = (0, Hx, 0)$. The equation for the electrostatic potential φ follows from the condition $\text{div} j = 0$ and one obtains

$$\frac{\partial^2 \varphi}{\partial x^2} + \frac{\partial^2 \varphi}{\partial y^2} = \rho_n \text{div} j_s, \quad (2)$$

where ρ_n is a normal-state resistivity and j_s is a superconducting current density.

Equation (1) is strictly valid only for gapless superconductors, but we use it here not to study the dynamics of Δ but to find the current at which the stationary superconducting state

[described by Eq. (1) with zero left-hand side (lhs)] becomes unstable. Equation (1) also provides the convenient way of finding the stationary state (if it exists at given current and magnetic field) starting from initial condition with $|\Delta|(x, y) = \Delta_{\text{GL}}(1 - T/T_c)^{1/2}$ and ending numerical calculations when the lhs of Eq. (1) goes to zero.

B. Results

In Fig. 2, we present the calculated $I_c(H)$ for the films with different widths. When $w \lesssim 6\xi$, in the film can exist only one vortex row at large H and there is one noticeable dip at $H = H^* \sim H_{c1}$ and one peak in dependence $I_c(H)$. For wider films, more than one vortex row may appear in the film [see dashed arrows in Fig. 2(b)] and each time when the new vortex row is nucleated in the film it leads to additional dips (and peaks) in dependence $I_c(H)$, but their amplitude is much smaller than for narrower films.

One can also notice short period oscillations of I_c well visible for relatively wide films at low magnetic fields [when in the film exists only one vortex row; see Fig. 2(b)] and for shorter films [see inset in Fig. 2(a)]. Their period ΔH depends on w and changes roughly from $\Delta H \simeq 1.3\Phi_0/wL$ for film with $w = 3\xi$ up to $\Delta H \simeq 1.9\Phi_0/wL$ for film with

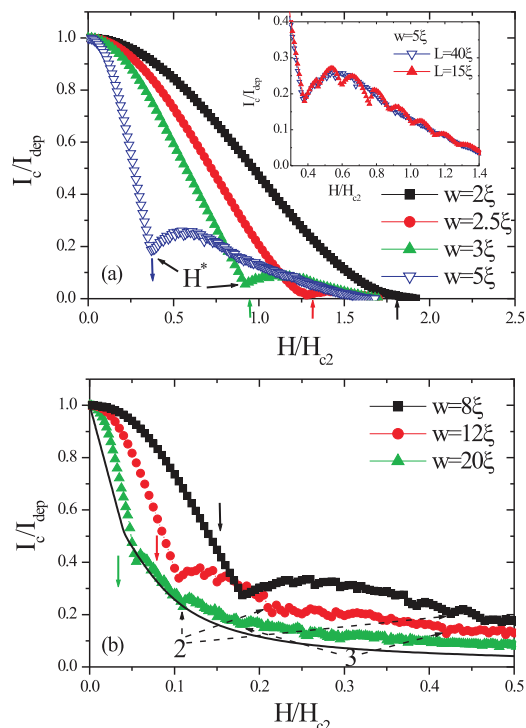


FIG. 2. (Color online) Dependence $I_c(H)$ for films with different widths and length $L = 40\xi$. Numbers and dashed arrows in (b) indicate the magnetic fields when second and third vortex rows appear in the film. Color arrows indicate the positions of H_{c1} for corresponding films. For relatively wide films $w \gtrsim 3\xi$, the critical current goes to zero at third critical magnetic field $H_{c3} \simeq 1.7H_{c2}$ when surface superconductivity vanishes. Black solid curve in (b) corresponds to theoretical $I_c(H)$ which follows from the London model [see Eqs. (23) and (37) in Ref. 20 or Eqs. (4) and (6) in Ref. 25] for film with $w = 20\xi$. Inset in (a) demonstrates the evolution of $I_c(H)$ when the length of the film decreases.

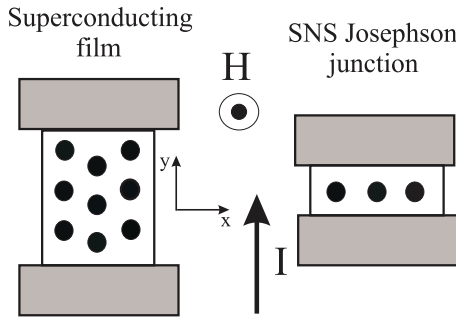


FIG. 3. Sketch of vortex distribution in the superconducting film and Josephson junction with finite length and width placed in the perpendicular magnetic field.

$w = 20\xi$ (Φ_0 is a magnetic flux quantum). These oscillations are connected with a change in the number of the vortices in the film by one and they are reminiscent of Fraunhofer-type oscillations of I_c in wide Josephson junction when the number of Josephson vortices changes by one. Similar oscillations were experimentally observed in mesoscopic single connected superconductors.⁴⁻⁷

It is interesting to note that qualitatively our results for evolution of $I_c(H)$ with increase of w resemble $I_c(H)$ for long diffusive Josephson junction of finite width [compare Figs. 2(a) and 2(b) with Fig. 3 in Ref. 53]. The difference is that in the Josephson junction, the number of the vortices changes by one (and it leads to appearance of new dips/peaks), while in the case of film the number of the vortex rows changes by one. The reason for such a difference is clear from Fig. 3. In the Josephson junction, there is only one vortex row which is *perpendicular* to the current, while in the film it could be several rows which are *parallel* to the direction of current flow. Besides, in the superconducting film, the number of the vortices in the row may vary with H , which provides an additional source of oscillations of $I_c(H)$ (mentioned in the previous paragraph). And, the last quantitative difference is that for the Josephson junction in the dips I_c goes to zero (see for example Ref. 53), while for narrow films it is finite there.

Let us now discuss why nonmonotonic behavior of $I_c(H)$ is the strongest one for relatively narrow films with $w \simeq 3-8\xi$ (we consider now the case of long films when short period oscillations have very small amplitude and may be discarded). In Fig. 4, we plot the current density distribution across the film at nonzero transport current and various H which follows from the London model in the vortex-free state. This current density is a sum of the transport current density $j_{tr} = I/wd$ and screening current density $j_{scr}(x) = -cHx/4\pi\lambda^2$. When sum $j_{tr} + j_{scr}$ on the left edge equals to the depairing current density j_{dep} , the superconducting state becomes unstable and vortices enter the film (in terms of energy barriers the barrier for vortex entry goes to zero on the left edge at this condition). These vortices may freely pass the film when $j_{tr} + j_{scr} > 0$ everywhere in the film (lines 1 and 2 in Fig. 4) because the Lorentz force $F_L = [j, \Phi_0]/c$ acting on the vortex directs to the right edge and the force from the vortex images $|F_{image}|$ is smaller than $|F_L|$ in the left half of the film. Keeping full current density at the left edge equal to j_{dep} and varying H , one can easily find linear decay $I_c(H) = I_c(0)(1 - H/H_s)$ (Ref. 20) at fields $0 < H < H_s/2$, where $I_c(0) = j_{dep}wd$ and H_s is a

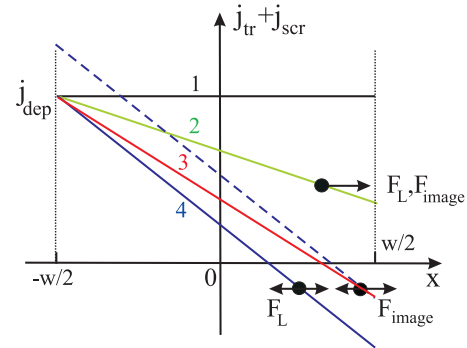


FIG. 4. (Color online) Sketch of current density distribution in narrow superconducting film. Black spot indicates the position of vortex and the forces which act on it. Line 1 corresponds to field $H^1 = 0$ and line 2 to $H^2 < H_s/2$. Lines 3 and 4 correspond to $H^3 > H^4 > H_s/2$. When $j_{tr} + j_{scr}$ changes the sign near the right edge of the film, the vortex stops in the point where $|F_L| = |F_{image}|$ (line 4). One needs to increase the current (dashed line) to move the vortex in the point where $|F_{image}| > |F_L|$ and the vortex can exit the film. The area under the lines determines the transport current in the film.

superheating magnetic field (at this field the surface barrier for vortex entry goes to zero at $I = 0$).

At field $H > H_s/2$, the sum $j_{tr} + j_{scr}$ changes the sign close to the right edge and the vortex would stop near this point because the Lorentz force changes the sign there. But, if this point is not far from the right edge, the force from vortex images is larger than the Lorentz force and the vortex is able to exit the film (line 3 in Fig. 4). At larger magnetic field, the vortex already can not leave the film (line 4 in Fig. 4) and one has to increase the current in the system to shift the vortex closer to the right edge in the point where $|F_{image}| > |F_L|$ (dashed line in Fig. 4). From Fig. 4, one can see that the area under the dashed line is larger than under line 3 and therefore the critical current is also larger. This consideration gives the physical background for increase of I_c at fields $H \gtrsim H_s/2$ (this explanation of peak effect is alternative to one present in Ref. 17).

In the above simple picture, we use the single-vortex approach (as in Ref. 17). But, when the barrier for vortex entry is suppressed, one will have not a single vortex but a vortex row with a period a which depends on applied magnetic field (see Figs. 5 and 6) [in the case $I = 0$ dependence $a(H)$ for film with $w = 5\xi$ is calculated in Ref. 16].

When the vortex row enters the film, it decreases the current density on the edge where it enters because the current which flows around the vortices j_{vort} has a different sign with current $j_{scr} + j_{tr}$. The vortex row stops at distance $r \sim w$ from left edge (left edge in Fig. 4 corresponds to bottom edge in Figs. 5 and 6) and hence reduction of j at that edge will be weaker for wider films $w \gg \xi$ in comparison with relatively narrow film where $w \sim \xi$ (see Fig. 6). Therefore, it is possible to have a situation that with the increase of the transport current the new vortices enter the film (when $j_{scr} + j_{tr} + j_{vort} \geq j_{dep}$) before the already existing vortex row exits the film and it launches the continuous vortex motion and resistive state. Our numerical calculations show that for relatively wide films, the resistive state starts according to this scenario (at least when in the film exists one vortex row). Then, it becomes clear that

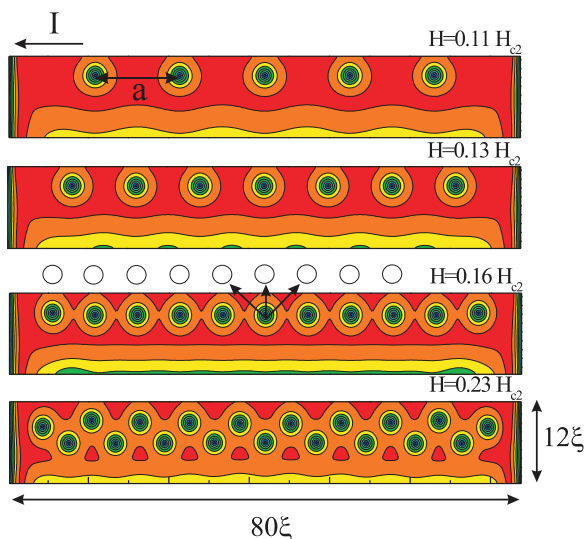


FIG. 5. (Color online) Distribution of $|\Delta|$ in the film with $w = 12\xi$ and $L = 80\xi$ at different magnetic fields and currents just below $I_c(H)$. One can see that already at $H \gtrsim H^* = 0.105H_{c2}$, the intervortex distance is smaller than the width of the film. The empty circles qualitatively demonstrate the position of the nearest vortex images and increased attraction to the edge due to the images of adjacent vortices.

the wider the film, the less one should increase I to create a new vortex row in the film and it explains the weak peak effect in films with $w \gg \xi$. In some respect, the situation is similar to mesoscopic samples with size (several $\xi \times$ several ξ) where oscillations of I_c are connected with compensation of the $j_{scr} + j_{tr}$ by j_{vort} and the amplitude of oscillations of $I_c(H)$ becomes small with increasing the length and width of the superconductor.

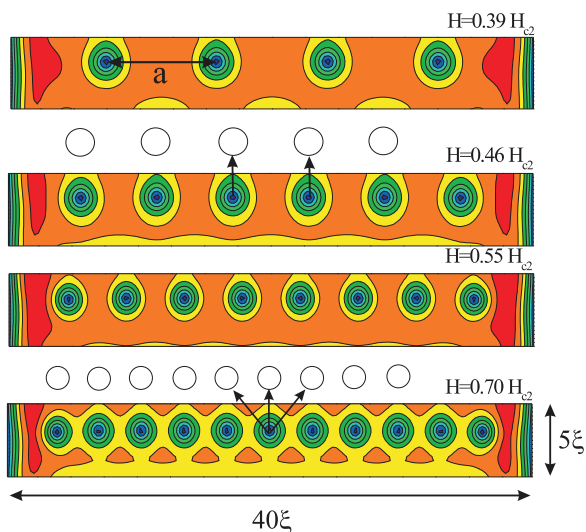


FIG. 6. (Color online) Distribution of $|\Delta|$ in the film with $w = 5\xi$ and $L = 40\xi$ at different magnetic fields and currents just below $I_c(H)$. The empty circles qualitatively demonstrate the position of the nearest vortex images. At relatively low H (when $a > w$), the main attraction to the edge comes from own image of the vortex, while at large H (when $a < w$) in addition there is noticeable attraction from images of adjacent vortices placed on distances less than w .

In films with $w \lesssim 10\xi$, our numerical calculations show that the resistive state at $H > H^*$ starts from the exit of the vortices, subsequent entry of new vortices, and so on. We believe that in such a film I_c grows up to the magnetic field at which the intervortex distance becomes about the width of the film. At larger fields when $a < w$, each vortex in the row stronger interacts with adjacent vortices and their images (at $a > w$ the vortex-vortex interaction decays exponentially with distance between vortices^{14,17}), which clearly enhances the attraction of the vortices to the nearest edge (see Fig. 6). The same effect exists in relatively wide films where even small increase of H above H^* leads to $a < w$ (see Fig. 5). In both cases, the enhanced trapping of vortex due to $j_{scr}(H)$ is compensated by increased interaction with the edge of the film due to smaller a , and when $a(H) < w$ the critical current decreases with increase of H . At large magnetic fields $H \simeq H_c$, additional decay of I_c comes also from suppression of $|\Delta|$.

We check that the peak effect is robust with respect of presence of the localized edge defects and suppression of the superconductivity along the edges. The last effect is discussed in Ref. 54 to explain the lowering T_c of the narrow films with decreasing their width. To model the localized edge defects, we locally suppress T_c in the semicircle with radius ξ placed at each edge (see inset in Fig. 7), while suppression of superconductivity along the whole edge of the film we model by reduction of T_c on distance of $\xi/4$ near the edges (see insets in Fig. 7 and Fig. 15). In both cases, this procedure leads to local suppression of $|\Delta|$ in the defect region and far from it (due to proximity effect, see inset in Fig. 7).

In Fig. 7, we present $I_c(H)$ for both types of defects (lower value of Δ_{edge} corresponds to lower value of local T_c). Suppression of T_s along edges shifts the position of the dip to larger fields which is explained by reduction of the effective “superconducting” width of the film [region which possesses the superconducting properties (see inset in Fig. 15)]. The

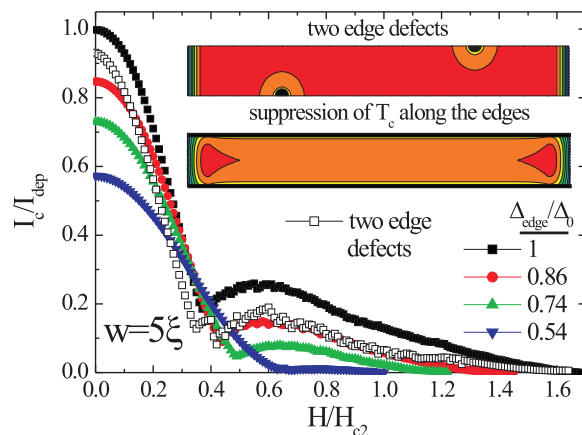


FIG. 7. (Color online) Dependence $I_c(H)$ for narrow film ($w = 5\xi$) with suppression of T_c along the edge leading to smaller value of the order parameter at the edge Δ_{edge} [it is normalized by $\Delta_0 = \Delta_{GL}(1 - T/T_c)^{1/2}$]. Curve with empty squares corresponds to the film with two localized edge defects (with chosen T_c^{loc} the minimum value of $|\Delta|$ in localized defect equals to $0.76 \Delta_0$). In the inset, we present distribution of $|\Delta|$ calculated at $H = 0$ and $I = 0$ for two types of suppression of T_c (regions with locally suppressed T_c are marked in black color).

localized edge defects lead to the appearance of two peaks (see curve with empty squares in Fig. 7). The first peak is connected with the single vortex localized near one of the edge defects (in the region between the defect and NS boundary) and second with a vortex row which appears at larger H . If one decreases T_c in the localized defect (which leads to a locally smaller value of $|\Delta|$), dependence $I_c(H)$ becomes irregular (not shown here) and it is hard to notice one pronounced peak. This could be explained by the presence of various widths (near localized defect the superconducting width of the film is effectively smaller) and peaks, which appear at different magnetic fields, and interfere with each other. It shows that the peak effect, in some respect, is a collective effect and to be observable one has to have relatively small variations of physical properties along the film.

C. Comparison with the London model

In this section, we compare our numerical results with those found in the London model.^{17–20} From Eqs. (18) and (20) of Ref. 17, one may find the position of the dip $H^* \simeq (H_s + H_0)/2$. It gives $H^* \simeq H_s/2$ for wide films $w \gg \xi$ ($H_0 \ll H_s$) and $H^* \simeq H_0 \sim H_{c1} \sim H_s$ when one approaches critical width w^* (where $H_0 \sim H_{c1} \sim H_s$) which qualitatively coincides with our numerical results. The amplitude of the peak and its position could not be found from the single-vortex approach used in Ref. 17.

In Refs. 18 and 19, the vortex-vortex interaction is taken into account in the framework of the the London model and calculated $I_c(H)$ demonstrates much higher peaks than our $I_c(H)$ for comparable width of the film ($w = 25\xi$) (see Fig. 2 in Ref. 18 and Fig. 9 in Ref. 19). Another quantitative difference is in the ratio of critical currents at $H = 0$ and at $H = H^*$. For moderately wide films $w \gtrsim 10\xi$, this ratio is about 2 in the GL model [see Fig. 2(b)] and in the single-vortex approach [it follows from Eqs. (18) and (20) in Ref. 17], while in Refs. 18 and 19 it was found $I_c(0)/I_c^{\text{dip}} \sim 10\text{--}20$.

Our $I_c(H)$ for the widest film ($w = 20\xi$) agrees semi-quantitatively with the result of Maksimova²⁰ [see black curve in Fig. 2(b)] for which we use $H_s = 0.083H_{c2}$ found from the GL model. The quantitative differences [nonlinear versus linear $I_c(H)$ at low H and larger values of $I_c(H)$ in the GL model at high H] are well explained by limitations of the London model. The nonlinear drop of I_c at low magnetic fields comes from suppression of $|\Delta|$ by the transport current in the GL model which is most noticeable when $I_c \sim I_{\text{dep}}$. This effect was previously discussed^{27,55} and experimentally confirmed in Ref. 55 for narrow Sn bridges. If due to some reason (for example presence of localized defects) I_c at zero magnetic field drops well below I_{dep} , one may recover the linear decay of I_c at low magnetic fields even in the GL model. The larger values of I_c in the GL model at high H come from the edge vortex-free layers with width about ξ (they provide finite I_c up to $H = H_{c3}$) and this effect can not be caught by the London model where formally $\xi \rightarrow 0$.

D. Comparison with the experiments

Experiments on narrow films with $\xi \ll w < \Lambda$ did not reveal presence of dips/peaks in $I_c(H)$ (Refs. 14, 23, and 24)

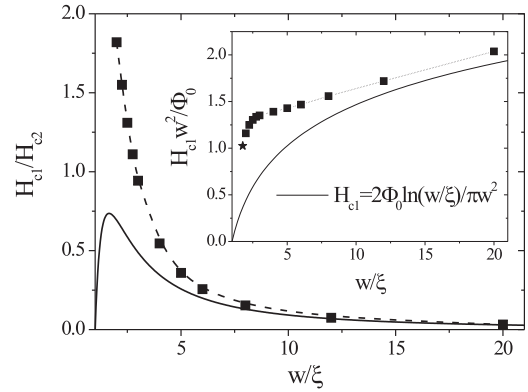


FIG. 8. Dependence of the first critical field H_{c1} (squares) on the width of the film found from the numerical calculations in the GL model. Black solid line follows from the London model (Refs. 17, 14, and 18). At $w = 2\xi$ field, H_{c1} is very close to the critical field H_c and we did not study more narrow films. The star in the inset corresponds to $H_{c1} = H_c$ for the film with $w = w^* \simeq 1.8\xi$ present in Ref. 8.

[the narrowest studied film had a width $w \simeq 14\xi$ (Ref. 23)]. Direct comparison with an analytical dependence following from the London model²⁰ showed good quantitative agreement between theory and experiment²⁴ at low magnetic fields where I_c linearly drops with H .

Narrow films with width $w \simeq 3\text{--}7\xi$ were experimentally studied in Refs. 21 and 22. In both experiments, $I_c(H)$ showed pronounced dips/peaks. Position of the first (single in Ref. 21) dip roughly follows $H = H^* \sim H_{c1}$ where dependence $H_{c1}(w)$ found in the GL model is shown in Fig. 8 (H_{c1} is found from the condition that at $H = H_{c1}$ the energies of the film with one vortex and vortex-free state are equal). Besides, the ratio $I_c(0)/I_c^{\text{dip}}$ extracted from Fig. 1 of Ref. 21 for the film with $w \simeq 4\xi$ (according to the table present in Ref. 21) is close to our value calculated for the film with $w = 4\text{--}5\xi$. It is more difficult to make the quantitative comparison with the results of Ref. 22 because of the logarithmic scale of shown dependence $I_c(H)$ and no information for actual width of the film in units of $\xi(T)$ at given temperature, but it is close to our results for the film with $w \sim 4\text{--}5\xi(T)$.

III. FIELD-DEPENDENT ENERGY BARRIER AND MAGNETORESISTANCE

In this section, we calculate the field-dependent energy barriers for vortex entry/exit to/from the narrow film when $I \rightarrow 0$. These results then are used to find the magnetoresistance of narrow films due to thermoactivated vortex hopping via these barriers.

A. Model

In Fig. 9, we illustrate hopping of the single vortex via energy barriers at different magnetic fields. At $H < H_0$, one needs to supply energy $U_{\text{en}}(H)$ to have a passage of the vortex across the film. Therefore, at fields less than H_0 finite resistance is proportional to $\exp[-U_{\text{en}}(H)/k_B T]$.

At fields larger than H_0 there is a local minimum in the dependence $U(x)$. Taking into account that vortex motion in the superconductors is strongly damped, one may conclude

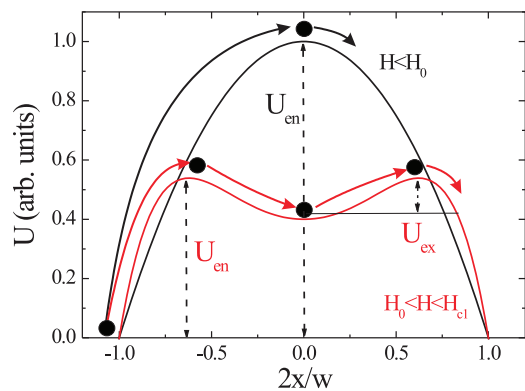


FIG. 9. (Color online) Sketch of the energy profile of the probe vortex placed in point x in the narrow film at magnetic fields $H < H_{c1}$.

that after overcoming the entry energy barrier, the energy of vortex will nearly follow the profile $U(x)$ and hence the vortex stops in the local minimum of $U(x)$. To exit the film, it should overcome the barrier U_{ex} and at the first sight the resistance at $H > H_0$ should be proportional to $\exp\{-[U_{en}(H) + U_{ex}(H)]/k_B T\}$ (which comes from the product of probabilities to enter and to exit the film). But, usage of the Arrhenius expression for estimation of vortex passage across the film implies that one should take into account not the sum of the barriers, but the maximal barrier. Indeed, let us suppose for definiteness that $U_{en} > U_{ex}$ (as in Fig. 9). Due to finite temperature, there is finite probability $P \sim \exp(-\Delta U/k_B T)$ to deliver energy ΔU in every part of the superconductor in each moment of time. When a fluctuation with the energy $\Delta U = U_{en}$ occurs near the edge, the vortex enters the film and then stops in the center. To exit the film, it needs smaller energy $\Delta U = U_{ex} < U_{en}$ and probability of such an event is much larger $\sim \exp(-U_{ex}/k_B T) \gg \exp(-U_{en}/k_B T)$ than for the vortex entry. Therefore, the largest barrier creates some kind of bottleneck and it determines the rate of vortex hopping across the entire film.

In the above consideration, one implicitly assumes that the pre-exponential factor gives the small contribution to the probability for vortex entry/exit. It is the case when $\Delta U/k_B T \gg 1$. In the opposite case, this simple approach becomes invalid and one has to calculate the pre-exponential factor and its dependence on ΔU .

In the vortex-free (Meissner) state $U_{en}(H) > U_{ex}(H)$ up to the field H_{c1} and probability for vortex entry $P_{en} \sim \exp[-U_{en}(H)/k_B T]$ is smaller than for the vortex exit $P_{ex} \sim \exp[-U_{ex}(H)/k_B T]$. Therefore, on average in time there are no vortices in the film at $H < H_{c1}$ (here we assume that the above probabilities are not extremely low and vortices can not be frozen in the film for very long times) and one may use the single-vortex approach for calculation of the energy barriers.

At fields larger than H_{c1} there are vortices in the film (because $P_{en} > P_{ex}$) and one has to take them into account. Again, we assume that to observe finite resistance in the experiment, the probabilities P_{en} and P_{ex} should not be extremely low. Consequently, for any magnetic field, the number of the vortices in the film is defined from the balance $P_{en} \sim P_{ex}$ which coincides with a condition that the film is being in the ground state. This assumption considerably

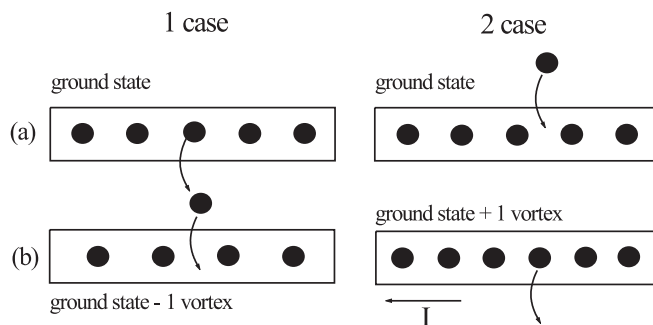


FIG. 10. Two scenarios of vortex passage through the film being in the ground state at $H > H_{c1}$. Case 1 has lower maximal energy barrier except near the magnetic fields where number of the vortices in the film changes by one in the ground state.

simplifies calculation of U_{en} and U_{ex} because one may consider only transitions from the ground state to the nearest metastable state (where the number of vortices is larger/smaller by one). But, even in this case there are two possibilities for thermoactivated vortex traveling across the film (see Fig. 10). Numerical calculations of the energy barriers show that in case 1 the maximal energy barrier corresponds to the barrier for exit (at $H > H_{c1}$), while in case 2 the maximal energy barrier corresponds to the barrier for entry (at $H > H_{c1}$) and it is larger than U_{ex} except near the magnetic fields at which the number of the vortices in the film changes by one in the ground state (see Fig. 11). Because of similar dependencies of $U_{max}(H)$ in both cases and mainly smaller value of U_{max} in case 1 than in case 2, we calculate the energy barriers for vortex hopping marked as case 1 in Fig. 10.

To calculate the energy barriers for vortex entry/exit, we numerically find the solution of the Ginzburg-Landau equation corresponding to the saddle-point (SP) state¹² at given value of magnetic field and number of vortices using the method of Ref. 11. For the vortex-free (Meissner) state, we place the probe vortex along the central line of the film [see Figs. 12(a) and 12(b)] and find profile $U(x)$ from which one can easily

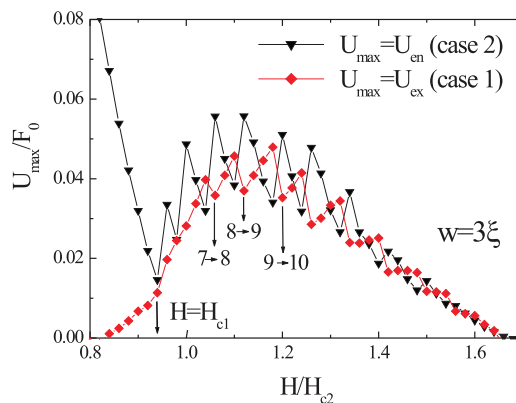


FIG. 11. (Color online) Dependence of the maximal energy barrier (at $H > H_{c1}$) for vortex entry/exit on magnetic field for two scenarios of vortex passage through the film (see Fig. 10). Numerics indicate the change in the number of the vortices in the film at corresponding magnetic fields. The width of the film is $w = 3\xi$ and the length is 40ξ . The energy is normalized in units of $F_0 = \Phi_0^2/8\pi^2\Lambda$.

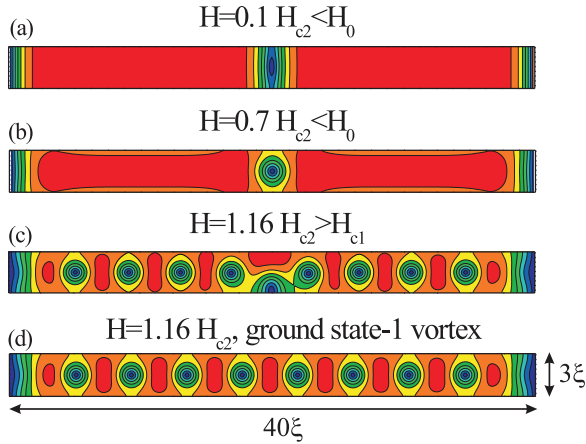


FIG. 12. (Color online) (a)–(c) Distribution of $|\Delta|$ in saddle-point state at different magnetic fields. In (d), we plot $|\Delta|$ in the metastable state which corresponds to state (b) of case 1 in Fig. 10.

extract U_{en} and U_{ex} . When the maximum of dependence $U(x)$ approaches the edge, then instead the vortex saddle-point state contains the vortex nucleus [finite-size region with partially suppressed $|\Delta|$ (Refs. 11 and 59)] sitting at the edge of the film. To find such a state, we fix the magnitude of the order parameter in one point of the numerical grid near the edge and vary $|\Delta|$ in this point (keeping H constant) until such a state becomes nonstationary and the vortex enters the film¹¹ (the same procedure is used for finding U_{ex} when we displace the vortex to the edge). The example of such a state is shown in Fig. 12(c).

By knowing both barriers, one can calculate the magnetoresistance using the expression

$$R(H) = \nu \exp(-U_{\text{max}}/k_B T), \quad (3)$$

where $U_{\text{max}} = \max\{U_{\text{en}}, U_{\text{ex}}\}$. Equation (3) contains the prefactor ν which can be found only from solution of the time-dependent problem.^{57,58} Its calculation for quasi-1D superconducting wire in the limit when fluctuations are rare events ($U/k_B T \gg 1$) showed that $\nu \sim (U/k_B T)^{1/2}$.^{57,58} But, when $U/k_B T \gg 1$ it is clear that the main dependence R on H comes from the exponent. Besides, when $H \rightarrow H_c$ and $U \rightarrow 0$ one should have normal-state resistance R_n . Therefore, for calculation (estimation) of magnetoresistance, we use the following semiphenomenological expression:

$$R(H) = R_n \exp(-U_{\text{max}}/k_B T). \quad (4)$$

B. Results

In Fig. 13, we present the dependence of maximal energy barrier $U_{\text{max}} = \max\{U_{\text{en}}, U_{\text{ex}}\}$ on the applied magnetic field for the films with widths $w = 2-5\xi$ (the energy is normalized in units of $F_0 = \Phi_0^2/8\pi^2\Lambda$). The maximal barrier corresponds to U_{en} at $H < H_{c1}$ and to U_{ex} at larger fields for vortex hopping marked as case 1 in Fig. 10. Similar to $I_c(H)$, there is a range of magnetic fields where U_{max} increases with increase of H [and hence R decreases according to Eq. (4)]. In the inset to Fig. 13, we show the high-field region for the film with $w = 3\xi$ where one can see that both barriers U_{en} and U_{ex} increase at $H > H_{c1}$. One can also notice short period oscillations of $U(H)$ [with practically the same period as for $I_c(H)$] which are connected

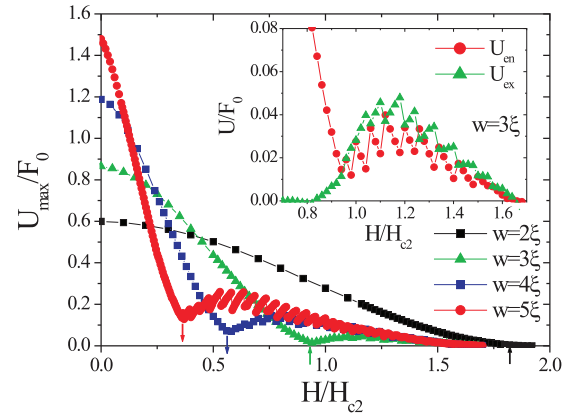


FIG. 13. (Color online) Dependence of the maximal energy barrier for vortex entry/exit on magnetic field for films with different width. In the inset, we plot both U_{en} and U_{ex} . Color arrows indicate field H_{c1} for given film. The length of the films is 40ξ .

with change in the number of the vortices. Due to the finite length of the film intervortex, the distance in the row changes discontinuously and it results in jumps of both U_{en} and U_{ex} . When the number of vortices is constant, both barriers vary continuously: U_{en} goes down and U_{ex} goes up because $j_{\text{scr}}(H)$ gradually increases when magnetic field grows.

For films with $w \gtrsim 8\xi$, the relative increase in $U_{\text{max}}(H)$ is much smaller than for narrower films (compare Figs. 13 and 14). In such films, the intervortex distance becomes comparable with w already at fields close to H_{c1} (see Fig. 15) and enhanced trapping of the vortices by j_{scr} is compensated by vortex-vortex repulsion and attraction by edges. In narrower films, $a(H) > w$ in a relatively wide range of magnetic fields [see Fig. 6, where the number of the vortices at $I \simeq I_c(H)$ is the same as at $I = 0$, contrary to film with $w = 12\xi$] and U_{ex} grows up to the field where $a(H) \lesssim w$ and at larger fields U_{ex} decreases. In addition, in relatively narrow films in which $H_{c1} \sim H_{c2}$, the order parameter is strongly suppressed in the film at $H \lesssim H_{c1}$ and the entrance of the vortex row increases

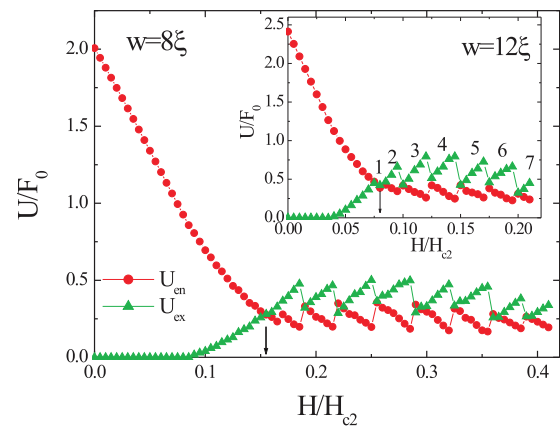


FIG. 14. (Color online) Dependence of U_{en} and U_{ex} on magnetic field for the film with $w = 8\xi$. In the inset, the results for the film with $w = 12\xi$ are present (numerics show the number of vortices at corresponding magnetic fields). The barriers are calculated up to the field when the second vortex row appears in the film. Arrows indicate field H_{c1} . The length of the films is 40ξ .

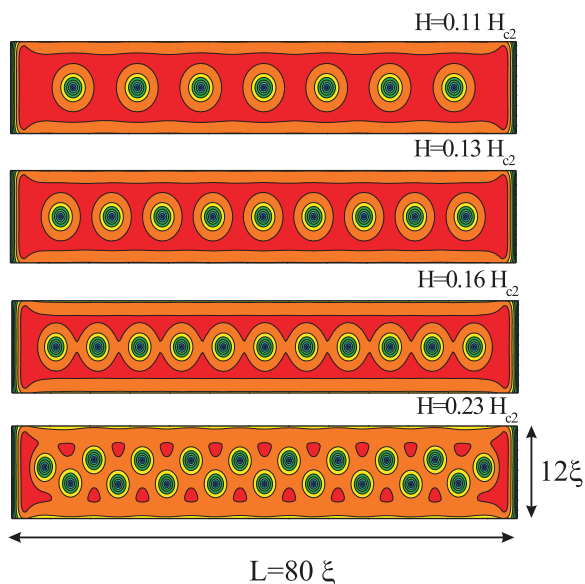


FIG. 15. (Color online) Distribution of $|\Delta|$ in the film with $w = 12\xi$ and $L = 80\xi$ being in the ground state at different magnetic fields [$I = 0$, compare it with Fig. 5 where $I \sim I_c(H)$].

$|\Delta|$ at the edge (due to compensation of j_{scr} by j_{vort}). It provides an increase of $U_{en}(H)$ in the film with $w = 3\xi$ (see inset in Fig. 13), but for wider films (where $H_{c1} \ll H_{c2}$) this effect is weaker.

Notice that the local minimum of $U_{max}(H)$ occurs at $H \simeq H_{c1}$ for all studied films ($w = 2-20\xi$) which is in contrast with dependence $I_c(H)$ for relatively wide films where the position of dip is shifted to larger magnetic fields [see Fig. 2(b)] and approaches $H_s/2$ when $w \gg \xi$. This result is not surprising because in relatively wide films where $H_{c1} \lesssim H_s/2$, the vortices are washed out from the film by the transport current at H_{c1} when $I \rightarrow I_c(H)$ (see discussion below Fig. 4) and the dip may appear only at larger fields.

C. Comparison with the London model

For relatively wide films, the energy barrier $U = U_{en}$ at $H < H_0$ decays almost linearly with H (see Fig. 14) which coincides with the predictions of the London model (see, for example, Refs. 14 and 20). For relatively narrow films, U_{en} decays nonlinearly with H which reflects the contribution of magnetic-field-dependent vortex core energy $U_{core}(H)$ to U_{en} (Ref. 11) (compare distribution of $|\Delta|$ in Fig. 12 at $H = 0.1H_{c2}$ and $H = 0.7H_{c2}$), while in the London model $U_{core}(H) = \text{const} \simeq 0.38F_0$.¹⁴

D. Comparison with the experiments

There are many works^{35-40,56} where measured $R(H)$ has a shape similar to the curve R^a in Fig. 1. There is simple criterion to distinguish to which of these results the present here theory could be relevant: according to our calculations, the first (or single) peak in $R(H)$ should occur at $H = H_{c1}$ which is shown in Fig. 8. References 35 and 38-40 relatively well fit this condition, but better agreement with a theory is reached when one uses a little smaller value of the width. Two more experiments^{36,37} also could be related to the present

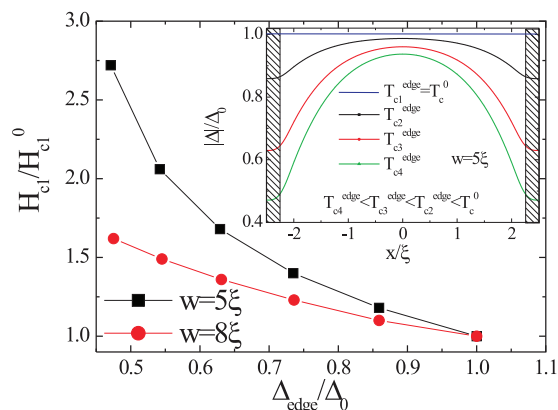


FIG. 16. (Color online) Dependence of H_{c1} for the films with nominal widths $w = 5\xi$ and 8ξ on the level of suppression of superconductivity near the edges due to locally smaller T_c . In the inset, we present distribution of $|\Delta|$ across the film for different T_c^{edge} at $H = 0$ and $I = 0$. Shaded areas mark the region where T_c is locally suppressed in our model.

theory although the peak in $R(H)$ occurs at considerably larger magnetic field $\sim 2.3H_{c1}$. It is interesting to note that in Refs. 36 and 37 different materials were used (Sn and a :InO correspondingly), but the first peak in $R(H)$ occurs almost at the same magnetic field for films with comparable widths [compare Fig. 3(b) in Ref. 36 with Fig. 2 in Ref. 37]. The main difference between these experiments is in the presence of short period oscillations in $R(H)$ observed in Ref. 37 and their period $\Delta H \sim 2\Phi_0/Lw$ is close to ours for film with $w \gtrsim 10\xi$.

As we show in Sec. II B, the locally smaller T_c along the edges shifts the position of the dip in dependence $I_c(H)$ to the larger fields. In Fig. 16, we demonstrate that H_{c1} increases when the order parameter near the edges decreases due to lower value of T_c . The effect is clearly stronger in relatively narrow film with $w = 5\xi$ where the decrease of the superconducting width by $\sim 2\xi$ (length scale of proximity effect) has a strong effect on H_{c1} . This result shows that smaller superconducting width than the real width of the film could be the reason for quantitative disagreement between the theory and the experiment.

Another source of quantitative discrepancy between the theory and some experiments may come from no rectangular geometry. In Ref. 35, the superconducting film was placed on the surface of cylinder, while in Ref. 38 the cylindrical nanowires were studied which raises a question about the effective width of such a sample and the correct value of H_{c1} .

Note that in some cases, a similar in shape dependence $R(H)$ can not be explained by vortex-assisted resistivity. For example, in Ref. 56 qualitatively similar dependence $R(H)$ was observed but the position of the peak occurs at $H \simeq 10^{-4}\Phi_0/w^2 \ll H_{c1}$ and we conclude that nonmonotonic $R(H)$ has a different origin.

In Fig. 17, we plot $R(H)$ which is calculated for parameters of tungsten film [$\xi(0) = 6$ nm, $\lambda(0) = 640$ nm, $w = 50$ nm, $d = 30$ nm] from Ref. 40 and where we assume Ginzburg-Landau temperature dependence for $\xi(T) = \xi(0)/(1 - T/T_c)^{1/2}$ and $\lambda(T) = \lambda(0)/(1 - T/T_c)^{1/2}$. We find the temperatures where the width of the film reaches 2ξ , 2.5ξ , 3ξ , 3.5ξ , and 4ξ and when inserted in Eq. (4) are

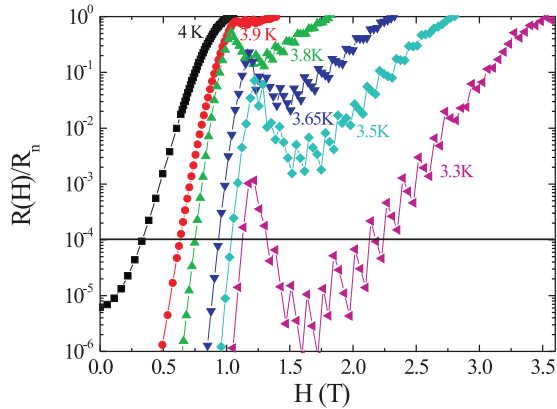


FIG. 17. (Color online) Magnetoresistance of the superconducting film with parameters of Ref. 40 calculated with the help of Eq. (4) and numerical results for $U_{\max}(H)$ (part of which is present in Fig. 13). $w = 2\xi(T)$ at $T = 4$ K and $w = 4\xi(T)$ at $T = 3.3$ K. Solid horizontal line shows the lowest measured resistance in Ref. 40.

numerically calculated as $U_{\max}(H)$ [parameter $F_0/k_B T$ varies from 20 at $T = 4$ K ($w = 2\xi$) up to 94 at $T = 3.3$ K ($w = 4\xi$)]. Note that at calculations we did not use any fitting parameters and nevertheless find qualitative agreement with the results of Ref. 40 [compare Fig. 17 with Fig. 2(a) from Ref. 40]. In Ref. 40, short period oscillations of $R(H)$ were not observed probably because of very large length of the sample $L \simeq 4 \mu\text{m} \simeq 670\xi(0)$. Quantitative agreement becomes better if one uses smaller width of the film in theoretical calculations [it shifts local maximum of theoretical $R(H)$ closer to experimental values and relative change of resistance at given temperature becomes closer to experimental findings].

IV. CONCLUSION

In the framework of the Ginzburg-Landau model, it is shown that transport properties (critical current I_c and resistance R due to thermoactivated vortex hopping via energy barriers at $I \ll I_c$) of long narrow superconducting films with width of about several ξ varies nonmonotonically with external magnetic field. Due to appearance of the vortex row in the film, the critical current increases and resistance decreases at $H \gtrsim H_{c1}$ until the intervortex distance in the row becomes smaller than w . At larger magnetic fields, I_c decreases while R increases. The effect is most strong in films with width $w \simeq 3-8\xi$. In wider films, already at fields when the first vortex row appears in the superconductor, the intervortex distance becomes less or comparable with w and the resulting effect is practically washed out due to vortex-vortex interaction.

Comparison with experiments demonstrates good qualitative agreement for position of the dip/peak in dependence $I_c(H)$ [$R(H)$] and in evolution of shape of $R(H)$ with temperature. Agreement becomes quantitative if one uses a smaller width of the superconductor, which looks reasonable if one assumes uniform (along the film) degradation of the superconducting properties (lower value of T_c) near the edges. This degradation weakly influences the existence of the peak effect and only shifts the position of the peak to larger fields and affects its amplitude.

Contrary, the variations of the physical properties (width and/or T_c) along the film have a destructive impact on the peak effect if these variations are relatively large. In such films, the minimum of $I_c(H)$ [maximum of $R(H)$] occurs at different fields $H^* \sim \Phi_0/w^2$ (corresponding to different superconducting widths in various parts of the film) and it smears out one well-pronounced dip/peak.

The finite length of the film produces additional short period oscillations both in $I_c(H)$ and $R(H)$ which are connected with discrete change in the number of the vortices. The amplitude of these oscillations decreases with increasing length of the film, but it is still noticeable for films with length 40ξ . The period of these oscillations is in quantitative agreement with the experimental findings of Ref. 37.

All present results are found in the framework of the GL model and are assumed to be quantitatively valid only close to T_c . But, we do not expect a large quantitative difference, and for lower temperatures (at least for “dirty” superconductors). For example, calculations of the energy barrier for the phase slip event in 1D superconductor at arbitrary temperatures (using the Usadel equation)⁶⁰ revealed a small difference with the result found in the GL model¹² [if one uses proper temperature dependence for $\xi(T)$ and $\lambda(T)$ at low temperatures]. Besides, both the peak effect and the negative magnetoresistance are most noticeable in relatively narrow films at fields $H \gtrsim H_{c1} \sim H_c$, and the order parameter at these magnetic fields is well suppressed below the equilibrium value which justifies, in some respect, the usage of the GL model at lower temperatures.

ACKNOWLEDGMENTS

The author thanks A. S. Mel’nikov and N. B. Kopnin for fruitful discussions. The author also thanks V. M. Vinokur for a very helpful dispute about the relation between the maximal energy barrier and probability for vortex passage across the superconducting film. The work was supported by the Russian Foundation for Basic Research (Project No. 12-02-00509) and by The Ministry of Education and Science of Russian Federation (Project No. 8686).

*vodolazov@ipmras.ru

¹W. A. Little and R. D. Parks, *Phys. Rev. Lett.* **9**, 9 (1962).

²V. L. Gurtovoi, S. V. Dubonos, A. V. Nikulov, N. N. Osipov, and V. A. Tulin, *Zh. Eksp. Teor. Fiz.* **132**, 1320 (2007) [*Sov. Phys.-JETP* **105**, 1157 (2007)].

³S. Michotte, D. Lucot, and D. Mailly, *Phys. Rev. B* **81**, 100503(R) (2010).

⁴D. Y. Vodolazov, F. M. Peeters, M. Morelle, and V. V. Moshchalkov, *Phys. Rev. B* **71**, 184502 (2005).

⁵N. Schildermans, R. Salenbien, A. V. Silhanek, and V. V. Moshchalkov, *Phys. C (Amsterdam)* **468**, 757 (2008).

⁶A. Falk, M. M. Deshmukh, A. L. Prieto, J. J. Urban, A. Jonas, and H. Park, *Phys. Rev. B* **75**, 020501 (2007).

- ⁷A. Yu. Aladyshkin, G. W. Ataklti, W. Gillijns, I. M. Nefedov, I. A. Shereshevsky, A. V. Silhanek, J. Van de Vondel, M. Kemmler, R. Kleiner, D. Koelle, and V. V. Moshchalkov, *Phys. Rev. B* **83**, 144509 (2011).
- ⁸D. Saint-James, G. Sarma, and E. J. Thomas, *Type II Superconductivity* (Pergamon, New York, 1969).
- ⁹K. K. Likharev, *Rev. Mod. Phys.* **51**, 101 (1979).
- ¹⁰C. Qiu and T. Qian, *Phys. Rev. B* **77**, 174517 (2008).
- ¹¹D. Yu. Vodolazov, *Phys. Rev. B* **85**, 174507 (2012).
- ¹²J. S. Langer and V. Ambegaokar, *Phys. Rev.* **164**, 498 (1967).
- ¹³A. A. Abrikosov, *Zh. Exp. Teor. Fiz.* **46**, 1464 (1964) [*Sov. Phys.-JETP* **19**, 988 (1964)].
- ¹⁴G. Stejic, A. Gurevich, E. Kadyrov, D. Christen, R. Joynt, and D. C. Larbalestier, *Phys. Rev. B* **49**, 1274 (1994).
- ¹⁵J. R. Clem, *Bull. Am. Phys. Soc.* **43**, 411 (1998).
- ¹⁶P. Sanchez-Lotero and J. J. Palacios, *Phys. Rev. B* **75**, 214505 (2007).
- ¹⁷V. V. Shmidt, *Zh. Eksp. Teor. Fiz.* **57**, 2095 (1969) [*Sov. Phys.-JETP* **30**, 1137 (1970)]. In that paper, the author studied the case of infinite (in two directions) superconducting plate (slab) with thickness $d < \lambda$ placed in a parallel magnetic field. In Refs. 14 and 20 it was argued that mathematically and physically this system is equivalent to the narrow thin superconducting film with width $w < \Lambda$ placed in a perpendicular magnetic field.
- ¹⁸Y. Mawatari and K. Yamafuji, *Phys. C (Amsterdam)* **228**, 336 (1994).
- ¹⁹G. Carneiro, *Phys. Rev. B* **57**, 6077 (1998).
- ²⁰G. M. Maksimova, *Phys. Solid State* **40**, 1607 (1998).
- ²¹L. P. Ichkitidze and V. I. Skobelkin, *Fiz. Niz. Temp.* **7**, 117 (1981) [*Sov. J. Low Temp. Phys.* **7**, 58 (1981)].
- ²²T. Yamashita and L. Rinderer, *J. Low Temp. Phys.* **24**, 695 (1976).
- ²³M. E. Gershenson and V. N. Gubankov, *Fiz. Tver. Tela* **21**, 700 (1979) [*Sov. Phys.-Solid State* **21**, 411 (1979)].
- ²⁴D. Henrich, P. Reichensperger, M. Hofherr, J. M. Meckbach, K. Ilin, M. Siegel, A. Semenov, A. Zotova, and D. Yu. Vodolazov, *Phys. Rev. B* **86**, 144504 (2012).
- ²⁵B. L. T. Plourde, D. J. Van Harlingen, D. Yu. Vodolazov, R. Besseling, M. B. S. Hesselberth, and P. H. Kes, *Phys. Rev. B* **64**, 014503 (2001).
- ²⁶D. Y. Vodolazov, B. A. Gribkov, A. Yu. Klimov, V. V. Rogov, and S. N. Vdovichev, *Appl. Phys. Lett.* **94**, 012508 (2009).
- ²⁷G. M. Maksimova, N. V. Zhelezina, and I. L. Maksimov, *Europhys. Lett.* **53**, 639 (2001).
- ²⁸A. A. Elistratov, D. Y. Vodolazov, I. L. Maksimov, and J. R. Clem, *Phys. Rev. B* **66**, 220506 (2002).
- ²⁹A. Rogachev, T.-C. Wei, D. Pekker, A. T. Bollinger, P. M. Goldbart, and A. Bezryadin, *Phys. Rev. Lett.* **97**, 137001 (2006).
- ³⁰M. Tian, N. Kumar, J. G. Wang, S. Y. Xu, and M. H. W. Chan, *Phys. Rev. B* **74**, 014515 (2006).
- ³¹T. C. Wei, D. Pekker, A. Rogachev, A. Bezryadin, and P. M. Goldbart, *Europhys. Lett.* **75**, 943 (2006).
- ³²M. Yu. Kharitonov and M. V. Feigelman, [arXiv:cond-mat/0612455](https://arxiv.org/abs/cond-mat/0612455).
- ³³D. Y. Vodolazov, *Phys. Rev. B* **75**, 184517 (2007).
- ³⁴G. R. Berdiyrov, X. H. Chao, F. M. Peeters, H. B. Wang, V. V. Moshchalkov, and B. Y. Zhu, *Phys. Rev. B* **86**, 224504 (2012).
- ³⁵R. D. Parks and J. M. Mochel, *Phys. Rev. Lett.* **11**, 354 (1963).
- ³⁶A. V. Herzog, P. Xiong, and R. C. Dynes, *Phys. Rev. B* **58**, 14199 (1998).
- ³⁷A. Johansson, G. Sambandamurthy, D. Shahar, N. Jacobson, and R. Tenne, *Phys. Rev. Lett.* **95**, 116805 (2005).
- ³⁸U. Patel, S. Avci, Z. L. Xiao, J. Hua, S. H. Yu, Y. Ito, R. Divan, L. E. Ocola, C. Zheng, H. Claus, J. Hiller, U. Welp, D. J. Miller, and W. K. Kwok, *Appl. Phys. Lett.* **91**, 162508 (2007).
- ³⁹J. Wang, Xu-Cun Ma, Li Lu, Ai-Zi Jin, Chang-Zhi Gu, X. C. Xie, Jin-Feng Jia, Xi Chen, and Qi-Kun Xue, *Appl. Phys. Lett.* **92**, 233119 (2008).
- ⁴⁰R. Cordoba, T. I. Baturina, J. Sese, A. Yu Mironov, J. M. De Teresa, M. R. Ibarra, D. A. Nasimov, A. K. Gutakovskii, A. V. Latyshev, I. Guillamon, H. Suderow, S. Vieira, M. R. Baklanov, J. J. Palacios, and V. M. Vinokur, *Nat. Commun.* **4**, 1437 (2013).
- ⁴¹P. Xiong, A. V. Herzog, and R. C. Dynes, *Phys. Rev. Lett.* **78**, 927 (1997).
- ⁴²M. L. Tian, N. Kumar, S. Y. Xu, J. G. Wang, J. S. Kurtz, and M. H. W. Chan, *Phys. Rev. Lett.* **95**, 076802 (2005).
- ⁴³Yu. Chen, S. D. Snyder, and A. M. Goldman, *Phys. Rev. Lett.* **103**, 127002 (2009).
- ⁴⁴Yu. Chen, Y.-H. Lin, S. D. Snyder, and A. M. Goldman, *Phys. Rev. B* **83**, 054505 (2011).
- ⁴⁵M. Zgirski, K.-P. Riikonen, V. Touboltsev, and K. Yu. Arutyunov, *Phys. Rev. B* **77**, 054508 (2008).
- ⁴⁶H. J. Gardner, A. Kumar, L. Yu, P. Xiong, M. P. Warusawithana, L. Wang, O. Vafek, and D. G. Schlom, *Nat. Phys.* **7**, 895 (2011).
- ⁴⁷D. A. Pesin and A. V. Andreev, *Phys. Rev. Lett.* **97**, 117001 (2006).
- ⁴⁸H. C. Fu, A. Seidel, J. Clarke, and D.-H. Lee, *Phys. Rev. Lett.* **96**, 157005 (2006).
- ⁴⁹K. Y. Arutyunov, *Phys. C (Amsterdam)* **468**, 272 (2008).
- ⁵⁰M. Y. Kharitonov and M. V. Feigel'man, *Zh. Eksp. Teor. Fiz.* **82**, 473 (2006) [*JETP Lett.* **82**, 421 (2005)].
- ⁵¹D. Y. Vodolazov, B. J. Baclus, and F. M. Peeters, *Phys. C (Amsterdam)* **404**, 400 (2004).
- ⁵²V. N. Gladilin, J. Tempere, J. T. Devreese, and V. V. Moshchalkov, *Phys. Rev. B* **86**, 104508 (2012).
- ⁵³J. C. Cuevas and F. S. Bergeret, *Phys. Rev. Lett.* **99**, 217002 (2007).
- ⁵⁴K. S. Il'in, M. Siegel, A. D. Semenov, A. Engel, and H. W. Hubers, *Inst. Phys. Conf. Ser.* **181**, 2895 (2004).
- ⁵⁵V. P. Andratskii, L. M. Grundel', V. N. Gubankov, and N. B. Pavlov, *Zh. Eksp. Teor. Fiz.* **65**, 1591 (1974) [*Sov. Phys. JETP* **38**, 794 (1974)].
- ⁵⁶K. A. Parendo, L. M. Hernandez, A. Bhattacharya, and A. M. Goldman, *Phys. Rev. B* **70**, 212510 (2004).
- ⁵⁷D. E. McCumber and B. I. Halperin, *Phys. Rev. B* **1**, 1054 (1970).
- ⁵⁸D. S. Golubev and A. D. Zaikin, *Phys. Rev. B* **78**, 144502 (2008).
- ⁵⁹V. A. Schweigert and F. M. Peeters, *Phys. Rev. Lett.* **83**, 2409 (1999).
- ⁶⁰A. V. Semenov, P. A. Krutitskii, and I. A. Devyatov, *Pis'ma Zh. Eksp. Teor. Fiz.* **92**, 842 (2010) [*JETP Lett.* **92**, 762 (2010)].